Available online at www.sciencedirect.com
SCIENCE DIRECT®

Journal of the European Ceramic Society 24 (2004) 1237–1241
www.elsevier.com/locate/jeurceramsoc

High temperature NTC ceramic resistors (ambient–1000 °C)

David Houivet*, Jérôme Bernard, Jean-Marie Haussonne

*LUSAC, Laboratoire Universitaire des Sciences Appliquées de Cherbourg (EA2607), Université de Basse Normandie, B.P.78,
50130 Cherbourg Octeville, France*

Abstract

New temperature sensors operating from ambient to 1000 °C, stable in diesel exhaust gas, and cheap, are needed. Such components may be ceramics. The value of their electrical resistance versus temperature is classically expressed as $R = a.\exp(B/T)$. Compounds from the ternary diagram Y_2O_3–Mn_2O_3–Cr_2O_3 may permit the obtaining of such performances. We have synthesized some compositions by solid-state reaction. Dense ceramics sintered at 1600 °C are two-phased, compound of a Y_2O_3 phase and an orthorhombic perovskite $YCr_{0.5}Mn_{0.5}O_3$ phase. Their resistivity at room temperature can be in the range 4 kΩ cm to 10^6 MΩ cm together with a B coefficient value of about 3600 K. Such ceramics can be used to make NTC resistors with a resistance value ranging from some hundreds kΩ at room temperature to some Ω at 1000 °C.

Keywords: Electrical properties; NTC; Perovskites; Thermistors; Y_2O_3

1. Introduction

The use of particle filters and catalytic converters in exhaust pipe for automotive motors involves to get temperature sensors operating from ambient to 1000 °C, stable in diesel gas, and cheap. Such components may be NTC ceramic resistors. NTC important electrical properties are the specific resistivity ρ, specified currently at 25 °C, the B value or energy constant of the material and the sensibility α. Resistance R measured at 25 °C provides the resistivity $\rho_{25\ ^\circ C} = RS/e$ with S the metallized surface and e the height when components have a cylindrical disc shape. B value is deduced from the Arrhenius equation $\rho(T) = \rho_{25\ ^\circ C}\exp(B/T)$ and thermistor sensitivity is defined by $\alpha = 1/\rho(d\rho/dT) = -B/T^2$. In order to make small NTC resistors with a resistance value ranging from some hundreds kΩ at room temperature to some Ω at 1000 °C, resistivities ranging from 1 to 100 MΩ cm and B values ranging from 2500 to 4500 K are required.

Classical ceramic NTC resistors composed of spinel structure (Mn,M,O_4) with M = Ni, Co, Fe, Cu, Zn show aging of the electrical properties and their application is commonly limited to temperatures below 200 °C. Rare earth oxide (Sm, Tb, Y ...) can be used for measurements at high temperature. The conduction of such oxides[1] is dependent on the atmosphere (p_{O2}) and densification. These effects can be limited by doping. Wang et al.[2] have studied the doping of Y_2O_3 by ZrO_2 and $CaZrO_3$ for NTC high temperature components. Their high resistivity (some MΩ at 800 °C) and B value around 24 000 K are not applicable for ambient to 1000 °C applications. Feltz and Pölzl[3] have proposed a system of compositions $Fe_xNi_yMn_{3-x-y}O_4$ based on the spinel structure for high temperature applications. Resistivities at 25 °C are ranging from 4.7 to 950 kΩ cm and B values from 3300 to 5000 K. Yet B values are not stable for temperatures below 400 °C, that limits the temperature range for applications. An other system, $Sr_xLa_{1-x}Ti_{x+y}Co_{1-x-y}O_3$ with perovskite structure, is proposed by one of these authors.[4] Resistivities at 25 °C are ranging from 1 Ω cm to 50 MΩ cm and B values from 1900 to 6900 K. These components synthesized by solid-state reaction and sintered at 1350 °C do not show aging phenomenon and could be used to applications from ambient to 1000 °C.

A Japanese patent[5] claims a system of composition $a(M_1M_2O_3)$–$b(Al_2O_3)$ with $0.05 < a < 1$ and $0 < b < 0.95$ ($a + b = 1$), M_1 = Y, Ce, Pr, Nd, Sm, Eu, Gd, Dy, Ho, Er, Yb, Mg, Ca, Sr, Ba, Sc, M_2 = Ti, V, Cr, Mn, Fe, Co, Ni, Zn, Al, Ga, Zr, Nb, Mo, Hf, Ta, W, in order to realize NTC thermistors ambient–1000 °C. The idea is to associate a less resistive phase with the perovskite structure $M_1M_2O_3$ with a high resistive phase Al_2O_3. Prompted by this pattern, we have studied the practic-

---

* Corresponding author.

0955-2219/03/$ - see front matter © 2003 Elsevier Ltd. All rights reserved.
doi:10.1016/S0955-2219(03)00376-5

ability and the electrical properties of compositions belonging to the system $a\mathrm{Y_2O_3}$-$b\mathrm{YCr_{0.5}Mn_{0.5}O_3}$•. The particular compound $\mathrm{YCr_{0.5}Mn_{0.5}O_3}$ is assumed to have a perovskite-type structure derived from $\mathrm{YCrO_3}$. Although the sintering behavior of $\mathrm{YCrO_3}$ has been reported as difficult in air,[6] its electrical properties and the effects of Mn substitution have been yet studied.[7] This single phase has a too high conductivity for our applications. So, by mixing with the more resistive phase $\mathrm{Y_2O_3}$ and according to the electrical properties mixing rules, we expect to obtain properties suitable for NTC applications from ambient to 1000 °C.

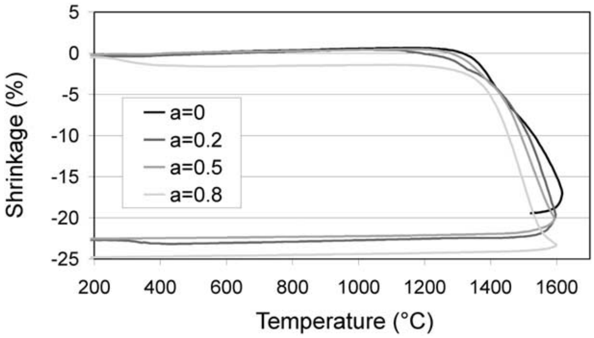

Fig. 1. Thermodilatometric curves, shrinkage versus temperature, of four compositions $a\mathrm{Y_2O_3}-b\mathrm{YCr_{0.5}Mn_{0.5}O_3}$.

2. Experimental

Different compositions $a\mathrm{Y_2O_3}$–$b\mathrm{YCr_{0.5}Mn_{0.5}O_3}$ were prepared by solid-state reaction, with $a = 0$, 0.2, 0.4, 0.5, 0.6, 0.7, 0.8 ($a + b = 1$). We mixed together reagent grade $\mathrm{Y_2O_3}$ (Aldrich 99.99%), $\mathrm{Cr_2O_3}$ (Aldrich 99%) and $\mathrm{Mn_2O_3}$ (Riedel-deHaën 99%) powders into an aqueous slurry by attrition milling for 1 h, using 0.8–1 mm zircon balls (SEPR ER120S). After drying, the mixed powders were calcined at 1200 °C. Calcined powders were mortar disagglomerated, 1 wt.% of an organic binder (Optapix®) was added and they were pressed at 175 MPa into 10 mm diameter and about 2.5 mm high cylindrical pellets. Pellets were sintered at 1600 °C for 5 h. The opposite sides of some sintered pellets were coated with a platinum paste and the components were fired at 1200 °C. Pure $\mathrm{Y_2O_3}$ pellets were also sintered and metallized in the same conditions.

Thermodilatometric measurements were performed up to 1600 °C with a Seteram TMA92 and density of sintered specimens was measured with a helium pycnometer Micromiretics Accupyc 1330. X-ray diffractometer Siemens D5005 using CuK_α radiation was used to identify crystalline phases in calcined powders and sintered ceramics. The microstructure was observed on polished surfaces using both an Olympus optical microscope and a Hitachi S2460N SEM. Phases compositions were investigated by EDS (Oxford Link Isis) operating at a 20 kV acceleration voltage. Resistances were measured from 25 to 1000 °C with Enertec 7150 digital multimeters. Resistances at 25 °C of compositions $a = 0.8$ and $\mathrm{Y_2O_3}$ were measured with a Sefelec SIM1000A megohmmeter.

3. Results and discussion

Thermodilatometric curves of different compositions $a\mathrm{Y_2O_3}$–$b\mathrm{YCr_{0.5}Mn_{0.5}O_3}$ are presented Fig. 1. For compositions with "a" < 0.5 ceramics are far to be full densified, since for $a = 0$ composition the shrinkage rate maximum is not reached at 1600 °C and just passed for $a = 0.2$ composition. On the other hand, 1600 °C sintering temperature seems to be sufficient for compositions with "a" ⩾ 0.5. So all compositions were sintered at 1600 °C for 5 h. The shrinkage of all specimens ranges from 14 to 20% and is reported in Table 1 together with measured densities of sintered pellets, and calculated porosities.

XRD patterns recorded on sintered pellets (Fig. 2) show, for all compositions with 0.2 ⩽ "a" ⩽ 0.8, two-phased ceramics. These two phases are present in different proportions in function of "a" value. They have been identified as $\mathrm{Y_2O_3}$ (JCPDF 41-1105 card) and an orthorhombic perovskite phase isomorphic to $\mathrm{YCrO_3}$ (34-035 card). For composition a = 0, corresponding to $\mathrm{YCr_{0.5}Mn_{0.5}O_3}$, the perovskite phase is alone. The cell parameters have been calculated from XRD pattern: $a = 5.640$ Å, $b = 7.478$ Å, $c = 5.257$ Å, and the calculated density is $D_x = 5.70$ corresponding to the

Table 1
Physical properties of sintered at 1600 °C compositions $a\mathrm{Y_2O_3}$–$b\mathrm{YCr_{0.5}Mn_{0.5}O_3}$

a ($\mathrm{Y_2O_3}$ mol%)	Vol ratio of $\mathrm{Y_2O_3}$	Shrinkage (%)	Density (measured)	Porosity (%)	$\rho_{25\ °\mathrm{C}}$ (Ω cm)	$B_{25/150\ °\mathrm{C}}$ (K)	$B_{700/1000\ °\mathrm{C}}$ (K)
0	0	13.8	5.70	18.8	$(4.4 \pm 0.3)10^{+04}$	3550 ±24	5950 ±500
0.2	0.25	16.9	5.56	10.5	$(1.95 \pm 0.06)10^{+05}$	3765 ±13	6300 ±500
0.4	0.47	18	5.41	4.8	$(3.4 \pm 1)10^{+05}$	3725 ±5	5750 ±500
0.5	0.57	19.1	5.31	4.7	$(1.6 \pm 0.8)10^{+06}$	3520 ±21	6200 ±500
0.7	0.76	19.8	5.16	2.4	$(4.2 \pm 0.3)10^{+07}$	3570 ±20	6300 ±500
0.8	0.84	19.8	5.11	2.4	$(1.3 \pm 0.5)10^{+12}$		21600 ±2000
$\mathrm{Y_2O_3}$	1	8.8	5.02	22.9	$(1.6 \pm 0.5)10^{+12}$		22700 ±2000

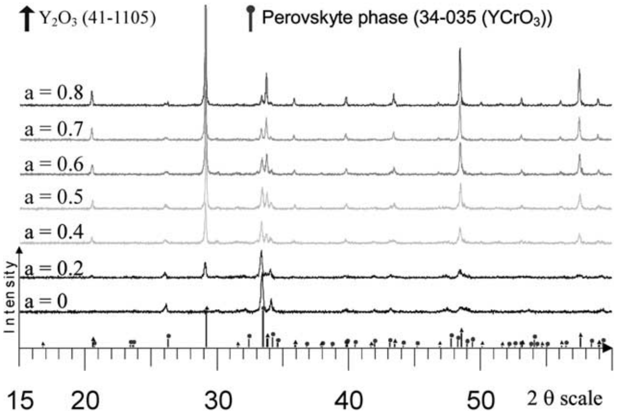

Fig. 2. XRD patterns of compositions $a\mathrm{Y_2O_3}$–$b\mathrm{YCr_{0.5}Mn_{0.5}O_3}$ sintered at 1600 °C.

measured value. Considering the $YCrO_3$ perovskite cell, Mn is assumed to substitute on the B-site of the ABO_3 perovskite lattice. The substitution of Mn^{3+} for Cr^{3+} induces a small increase of the volume cell (221.7 Å^3 instead of 218.2 Å^3 for $YCrO_3$). Such increase is in agreement with the difference of ionic radius of Cr^{3+} and Mn^{3+} (0.62 and 0.65 Å, respectively). No order phenomenon was detected by XRD compared to simulated diagrams.

Microstructural observations confirm the obtaining of two-phased ceramics. In Fig. 3, optical micrographies of different compositions are presented. The phases contrast is obvious: the Y_2O_3 phase appears as gray and the other phase appears as white. These two phases seem to be well dispersed into the ceramics with grains size

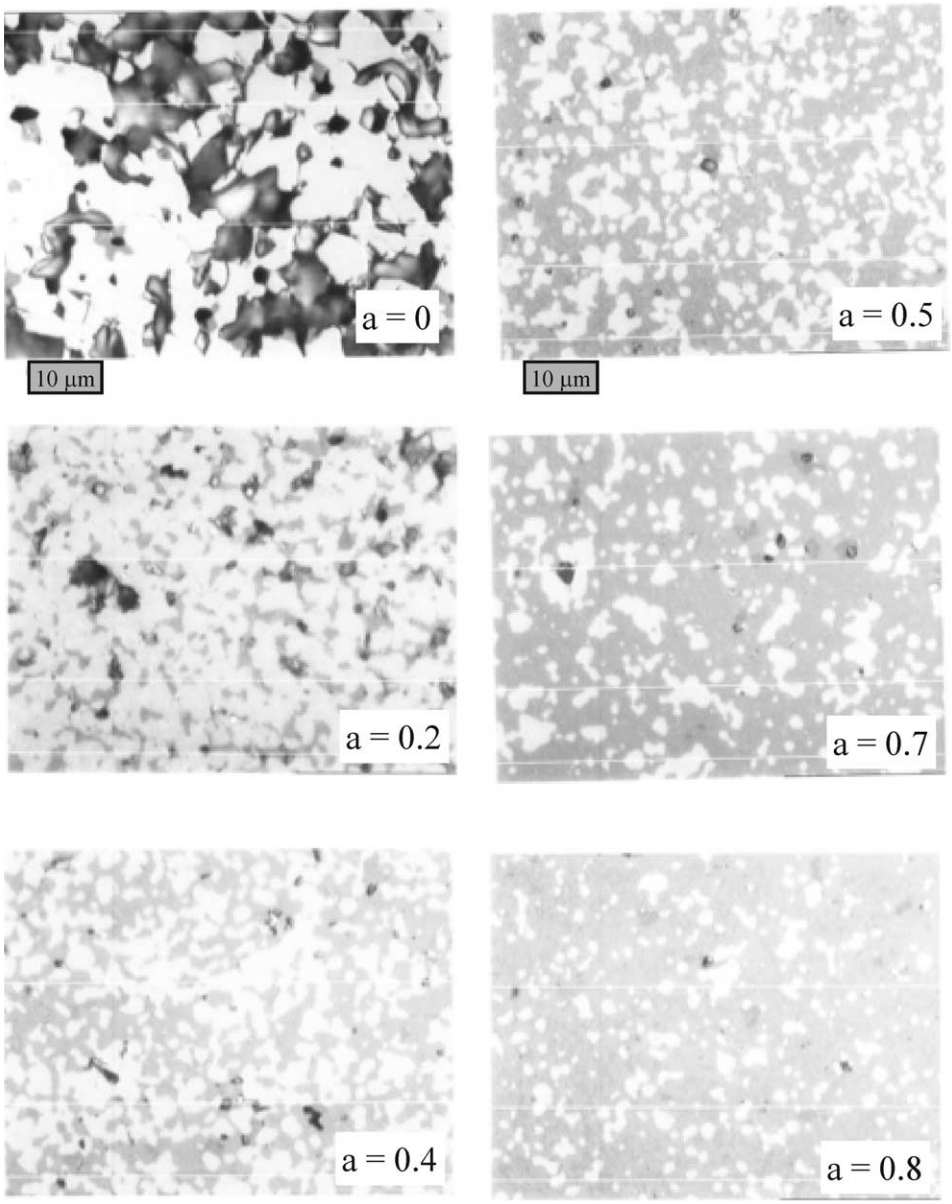

Fig. 3. Optical micrographies of sintered and polished specimens for different compositions.

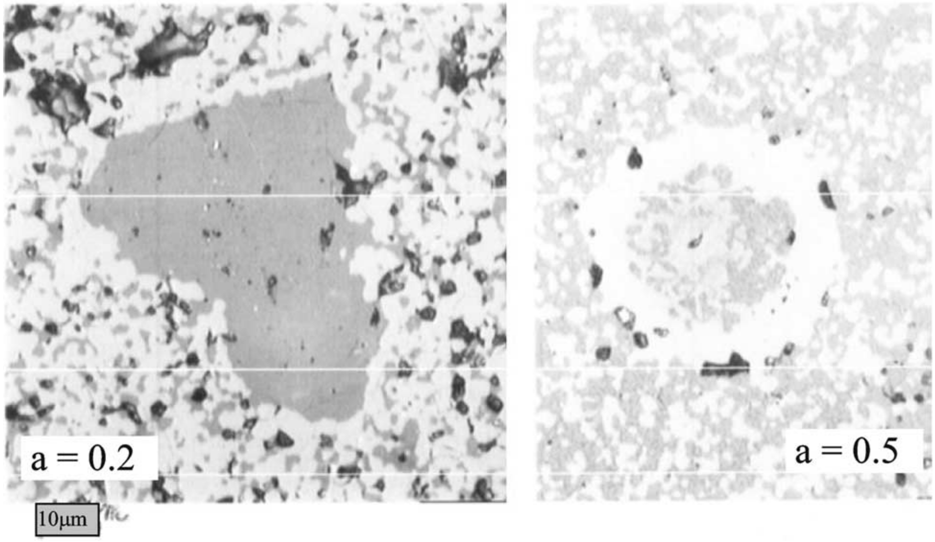

Fig. 4. Optical migrographies of some phases dispersion defaults.

smaller than 2 µm. Yet, some rarely observed defaults of the two phases dispersion are shown Fig. 4. Some grains of the same phase can gather together. For the composition $a=0$, we can observe lot of porosity together with the white phase. Global EDS analyses of ceramics are equivalent to the prepared compositions (in the limit of the analysis error), that is to say not any notable evolution of composition occurs during the sintering cycle. The pointed EDS analyses confirm two main phases whatever the "*a*" value, one with chemical composition more than 98% Y_2O_3 and the other with composition near to $YCr_{0.5}Mn_{0.5}O_3$. Notice that a third phase, in very small quantity undetectable by XRD, with composition near to $Y_{0.8}Cr_{0.1}Mn_{0.1}O_3$ can be also observed whatever "*a*".

As we confirm with both XRD and EDX analyses that the two main phases present in ceramics are Y_2O_3 and the perovskite phase $YCr_{0.5}Mn_{0.5}O_3$, we can expect, in the case of a phase mixing without solid solution, that the molar relative proportion of these two phases is very close to the "*a*" value. This is confirmed by the variation of ceramic densities that is conform to a single mixing phase rule.

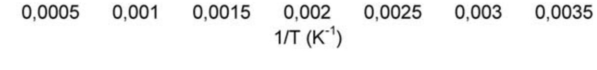

Fig. 5. ln(Resistivity ρ) for aY_2O_3–$bYCr_{0.5}Mn_{0.5}O_3$ as a function of $1/T$.

For all compositions, electrical resistances of Pt metallized cylindrical pellets with a diameter of about 8 mm and a height of about 2.2 mm were measured. Resistance *R* measured at 25 °C provides the specific electrical resistivity $\rho_{25\ ^\circ C}$. We notice that the dispersion on the measured resistivities for different pellets of the same composition is greater than the error due to measurement apparatus. This is the consequence of the presence of ceramic defaults as microcracks, porosity, or yet cited phases dispersion. Measurements from 25 to 1000 °C provide the *B* value. These measurements are reported in Fig. 5 as Ln(ρ) as a function of $1/T$. We can observe that the plotting curves are not linear on the wide temperature range, which highlight two conduction phenomena, the first from ambient to 700 °C and the other activated after 700 °C. So we have calculated by least square refinement two *B* values (data in Table 1) the one for temperature ranging from 25 to 150 °C ($B_{25/150\ ^\circ C}$) and the second from 700 to 1000 °C ($B_{700/1000\ ^\circ C}$). Evolution of resistivities and *B* values as a function of "a" is plotted in Fig. 6. Resistivities at 25 °C and at 700 °C slightly increase with "*a*" up to 0.7. There is a gap between 0.7 and 0.8. *B* values are stable for "a" $\leqslant 0.7$, with values around 3600 K for the $B_{25/150\ ^\circ C}$ and 6000 K for the $B_{700/1000\ ^\circ C}$. Such *B* values are far to these presented in the Denso pattent,[5] 2170 K for $YCr_{0.5}Mn_{0.5}O_3$ and 2580 for $38YCr_{0.5}Mn_{0.5}O_3$-$62Y_2O_3$. For "*a*" $\geqslant 0.8$, $B_{700/1000\ ^\circ C}$ value become greater than 20 000K.

It seems that two Maxwell mixing rules control the electrical properties, with $YCr_{0.5}Mn_{0.5}O_3$ phase as matrice for "*a*" $\leqslant 0.4$ (corresponding to a 50% volume ratio) and with Y_2O_3 phase as matrice for "*a*" $\geqslant 0.8$.

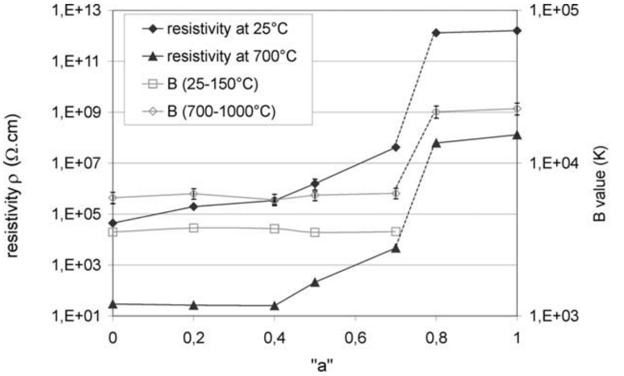

Fig. 6. Evolution of resistivities at 25 and 700 °C and *B* values as a function of the molar ratio“*a*”.

Between 0.4 < ”*a*” < 0.8 the electrical behavior seem to be controlled by a percolation phenomenon. These considerations will be discussed elsewhere. So, the microstructure, the dispersion of the two phases, the grains size…, in fact the ceramic processing will thus be of first importance in order to control electrical properties, the reproducibility and the reliability of NTC components.

4. Conclusions

Different ceramic compositions aY$_2$O$_3$–bYCr$_{0.5}$Mn$_{0.5}$O$_3$ ($a+b=1$) were prepared by solid-state reaction. The microstructure is two-phased, compound of a Y$_2$O$_3$ phase and an orthorhombic perovskite YCr$_{0.5}$Mn$_{0.5}$O$_3$ phase. Electrical resistivities $\rho_{25\ °C}$ range from 4.10^{+04} to 10^{+12} Ω.cm depending on “*a*” value. $B_{25/150\ °C}$ is around 3600K whatever “*a*” value lower than 0.7. Such ceramics, with 0.5 < ”*a*” < 0.7, can be used to make small NTC thermistors with a resistance value ranging from some hundreds kΩ at room temperature to some Ω at 1000 °C. Further works will be concentrated on ceramic processing that seem to have influence on electrical properties, on the aging of such components in different atmospheres, and on the possibility to modulate the *B* value.

Acknowledgements

The authors would like to thank M. Lemariey for ceramic preparation. This study is supported by European funds FEDER

References

1. Banerjee, A. and Akbar, S. A., A new method for fabrication of stable and reproductible yttria-based thermistors. *Sensors and Actuators A*, 2000, **87**, 60–66.
2. Wang, C. C., Akbar, S. A., Chen, W. and Schorr, J. R., High-temperature thermistors based on yttria and calcium zirconate. *Sensors and Actuators A*, 1997, **58**, 237–243.
3. Feltz, A. and Pölzl, W., Spinel forming ceramics of the system Fe$_x$Ni$_y$Mn$_{3-x-y}$O$_4$ for high temperature NTC thermistor applications. *J. Eur. Ceram. Soc.*, 2000, **20**, 2353–2366.
4. Feltz, A., Perovskite forming ceramics of the system Sr$_x$La$_{1-x}$Ti$_{x+y}$Co$_{1-x-y}$O$_3$ for NTC thermistor applications. *J. Eur. Ceram. Soc.*, 2000, **20**, 2367–2376.
5. Itusuhei, O., Nasanori, Y., Eturo, Y. and Kaoru, K., *Dispositif de thermistance, methode de fabrication d'un tel dispositif et capteur de temperature*. Denso Corporation, French paten FR 9902475, 26 February. 1999.
6. Lambert-Bates, J., Chick, L. A. and Weber, W. J., Synthesis, air sintering and properties of lanthanum and yttrium chromites and manganites. *Solid State Ionics*, 1992, **52**, 235–242.
7. Weber, W. J., Griffin, C. W. and Lambert-Bates, J., Effects of cation substitution on electrical and thermal transport properties of YCrO$_3$ and LaCrO$_3$. *J. Am. Ceram. Soc.*, 1987, **70**(4), 265–270.